Macromolecules
ARTICLE

Macromolecules **2010**, *43*, 9077–9086 **9077**
DOI: 10.1021/ma102027t

Reversible Hierarchical Phase Separation of a Poly(methyl methacrylate) and Poly(*n*-nonyl acrylate) Blend in a Langmuir Monolayer

Yuhtaro Sasaki,[†,§] Naoyuki Aiba,[†,⊥] Hiroshi Hashimoto,[†] and Jiro Kumaki*[,†,‡]

[†]*Department of Polymer Science and Engineering, Faculty of Engineering, Yamagata University, Yonezawa, Yamagata 992-8510, Japan, and* [‡]*Department of Polymer Science and Engineering, Graduate School of Science and Engineering, Yamagata University, Yonezawa, Yamagata 992-8510, Japan.* [§]*Present address: Miyako Branch, Tohoku Bank, 2-25 Aramachi, Miyako 027-0086, Japan.* [⊥]*Present address: Material Technology Research and Development Laboratories, Tokai Rubber Industries, Ltd., 3-1 Higashi, Komaki 485-8550, Japan*

Received September 1, 2010; Revised Manuscript Received October 1, 2010

ABSTRACT: Mixed Langmuir monolayers composed of poly(methyl methacrylate) (PMMA) and poly(*n*-nonyl acrylate) (PNA) were studied by surface pressure−area isotherms and atomic force microscopy (AFM). The mixed monolayer was miscible at a low surface pressure but underwent a reversible hierarchical phase separation at a high surface pressure, with the monolayer of the major component being spread on the water surface, on top of which the minor component separated out. The phase separation grew with time, but upon reduction of the surface pressure into the miscible region, the phase separation immediately disappeared. A subsequent increase of the surface pressure into phase separation region again caused a phase separation similar to that from the miscible state, indicating that the blend monolayer converted to the original miscible state immediately upon reduction of the surface pressure. Thus, this hierarchical phase separation is completely reversible and a true thermodynamic transition. A PMMA-*b*-PNA block copolymer also showed a similar reversible hierarchical phase separation, with the major component being spread on the water surface, on top of which the minor component again separated out. The domain size was regular, corresponding reasonably well to the chemical structure of the block copolymer, and did not grow with elapsed time.

1. Introduction

Polymer monolayers spread on a water surface are superior in mechanical and thermal stability in comparison with monolayers composed of small molecules, and thus, they have been extensively studied for possible applications as functional thin films.[1] Polymer monolayers are also an ideal model for the study of polymer chains in two-dimensional (2D) states, and the structure and properties of such 2D states are also the subject of intense study. Polymer blend monolayers have also been studied.[2−20] The miscibility of polymer blends in 2D states might be different from that in 3D states, since interaction between blended polymers in the monolayer is different from those in 3D states because of specific alignments of the monomer units of the polymer in the monolayer as a result of adsorption of a hydrophilic group in the monomer unit onto the water surface.[2,8,10] In addition, the contribution of interfacial free energy of the water/monolayer and air/monolayer interfaces should be considered in the 2D films. Further, polymer chain packing in 2D states, which are different from those in 3D states,[21] may also affect the miscibility and the resultant morphology of polymer blends in the monolayers.

In the earlier studies, the miscibility of polymer blends in monolayers was mainly identified from the surface pressure−area ($\pi-A$) isotherms[2,4−10,17,19] as follows. If a plot of the area versus the composition of a blend at a constant surface pressure was linear, in other words, the area obeyed an additive rule, the blend was regarded as miscible or perfectly immiscible. A negative deviation of the area from the additive rule was considered evidence for an attractive interaction between the component polymers; therefore, the polymer blend was identified as miscible. On the other hand, a positive deviation of the area from the additive rule was thought to indicate the existence of a repulsive interaction between the component polymers. In addition to the area−composition relationship, the dependence of the collapse pressure on the composition of the blend was also thought to be evidence of the miscibility of the blends. On the other hand, for a completely immiscible mixture, the collapse pressure was expected to be independent of the composition. The miscibility of many polymer blend monolayers was identified in this manner, for example: poly(methyl methacrylate) (PMMA)/poly(vinyl acetate) (PVAc),[2,10,11] PMMA/poly(ethyl methacrylate) (PEMA),[4,6] PEMA/poly(butyl methacrylate) (PBMA),[5,6] PMMA/PBMA,[6] cellulose acetate/poly(dimethylsiloxane),[7] binary blends selected from PMMA, PVAc, poly(propyl methacrylate), poly(vinyl stearate), and poly(octadecyl methacrylate),[8] poly(phenyl methacrylate) with poly(hexyl methacrylate) or poly(benzyl methacrylate),[9] poly(ethylene oxide) (PEO)/PMMA,[10] poly(methyl acrylate)/PVAc,[10,12] PEO/PVAc,[10] PMMA/poly(vinylphenol),[17] and poly(*n*-butyl methacrylate) blends with its isomers (poly(isobutyl methacrylate), poly(*sec*-butyl methacrylate), and poly(*tert*-butyl methacrylate)).[19]

In contrast, in 3D states, the miscibility of polymer blends is determined mainly by more direct measurements, for example, microscopies, such as optical and transmission/scanning electron microscopy (TEM, SEM), scattering techniques, such as light, X-ray, and neutron scattering, and thermal analysis by differential scanning calorimetry (DSC), etc. Thus, in order to study miscibility of blend monolayers, a $\pi-A$ isotherm measurement may not be sufficient and a morphological investigation may be necessary. Therefore, in limited cases, some other measurements have been used in addition to the $\pi-A$ isotherms, for example,

*To whom corresponding should be addressed. E-mail: kumaki@yz.yamagata-u.ac.jp.

Published on Web 10/13/2010

ellipsometry of the thickness and refractive index of mixed monolayers,[11] Brewster angle microscopy (BAM)[18] and fluorescence microscopy[16] of monolayers on the water surface, SEM of collapsed monolayers,[9] TEM[14] and scanning near-field microscopy (SNOM)[14] of monolayers deposited on substrates. At present, atomic force microscopy (AFM) is one of the best tools to observe monolayers. Polymer monolayers have been observed by AFM at a molecular level[22−27] and thus is frequently used for studying blend monolayers in combination with the $\pi-A$ isotherm measurement.[12,13,16,20]

Previously, we studied the miscibility and stereocomplex formation between isotactic and syndiotactic poly(methyl methacrylate)s (it- and st-PMMA) in the monolayers on a water surface by $\pi-A$ isotherm measurements and AFM.[20] We found that at a normal compression rate it- and st-PMMA phase separated, and upon further compression, a stereocomplex was formed only at the interface of it- and st-PMMA domains. On the other hand, at a 1/50 slower compression rate than the normal, an it- and st-PMMA mixture formed a miscible monolayer, and further compression resulted in quantitative stereocomplex formation. The apparent immiscibility of the mixture was kinetically controlled, since it-PMMA and st-PMMA form an expanded and condensed monolayer, respectively, in a dilute state;[22] they are therefore immiscible when dilute. At a faster rate of compression, the phase separation seen in the dilute state was retained, resulting in the apparent phase-separated structure. These complicated behaviors of compression-rate-dependent phase separation and stereocomplex formation could be fully analyzed by the combination of $\pi-A$ isotherm measurement and AFM.

In this paper, we report a study of a mixed monolayer composed of PMMA and poly(*n*-nonyl acrylate) (PNA) by $\pi-A$ isotherm measurements and AFM. Upon compression, the monolayer formed a hierarchical phase separation, with the major component spread on the water surface as a monolayer, on top of which the minor component separated out. Detailed AFM observations indicated that the mixed monolayer was miscible at a low surface pressure, and the hierarchical phase separation was reversibly formed at a high surface pressure. Depending on the composition, the lower monolayer of the hierarchical phase separation was either PMMA or PNA, and at a PNA-rich composition, phase inversion of the upper and lower layer of the once-formed hierarchical phase separation occurred upon further compression. These complicated phase separation behaviors were fully analyzed using a combination of $\pi-A$ isotherm measurements and AFM.

2. Experimental Section

2.1. Materials. The PMMA and PNA used in this study were purchased from Showa Denko (Tokyo, Japan) and Polymer Source (Montreal, Canada), respectively. The number-average molecular weights (M_n) and molecular weight distributions (M_w/M_n) were 1.96×10^4 and 1.03 for the PMMA and 1.3×10^4 and 1.50 for the PNA, respectively. The PMMA-*b*-PNA was also purchased from Polymer Source. The M_n for the PMMA and PNA blocks were 1.3×10^4 and 2.03×10^5, respectively, and the M_w/M_n was 1.25. Highly purified benzene (Infinity Pure, Wako Chemicals, Osaka, Japan) was used as the solvent for the spreading solutions without further purification. Water was purified by a Milli-Q system and used as the subphase for the LB investigations.

2.2. Surface Pressure−Area ($\pi-A$) Isotherm Measurements and LB Film Preparations for AFM. The $\pi-A$ isotherm measurements of a PMMA, PNA, their mixtures (PMMA/PNA = 25/75, 50/50, and 75/25 in weight fraction), and a PMMA-*b*-PNA were done as follows: A PMMA, PNA, their mixture, or a PMMA-*b*-PNA solution in benzene having a total polymer concentration from 2×10^{-4} to 6×10^{-5} g/mL was spread on a water surface at 25 °C in a commercial LB trough with an area of 60×15 cm^2 and an effective moving barrier length of 15 cm (FSD-300AS, USI, Japan). The surface pressure was measured using filter paper as the Wilhelmy plate. The $\pi-A$ isotherms were measured at a constant compression rate with a moving barrier speed of 0.5 mm/s. A monolayer was deposited onto a piece of freshly cleaved mica by pulling it out of the water at a rate of 4.2 mm/min, while compressing the monolayer at a constant pressure (the vertical dipping method).

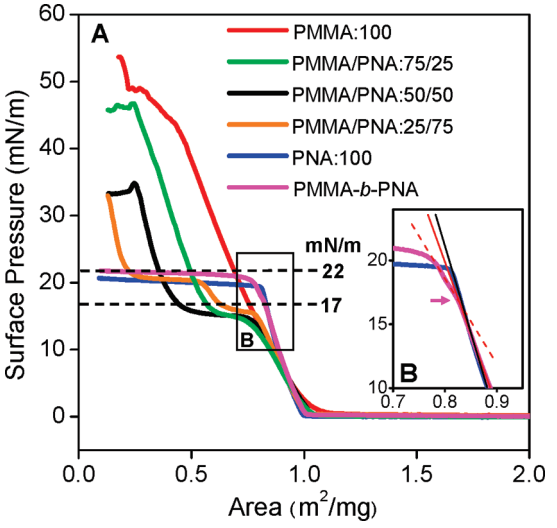

Figure 1. (A) $\pi-A$ isotherms of monolayers of PMMA, PNA, PMMA/PNA mixtures, and PMMA-*b*-PNA on water. (B) Magnified $\pi-A$ isotherms of monolayers of PNA (blue) and PMMA-*b*-PNA (pink) at the region indicated by the square (B) in (A).

In order to evaluate the reversibility of the $\pi-A$ isotherms, a monolayer was first compressed up to a prescribed surface pressure (first compression), then expanded to 2.0 m^2/mg (0 mN/m), and again immediately compressed (second compression). Also, the monolayer was deposited at constant surface pressures by the vertical dipping method during a compression−expansion−compression cycle and observed by AFM. The compression and expansion rates for the reversibility investigation were 0.5 mm/s.

2.3. AFM Observations. After drying the deposited monolayers in vacuo, they were observed by a commercial AFM (NanoScope IIIa or IV/multimode AFM unit, Veeco Instruments, Santa Barbara, CA) with standard silicon cantilevers (PointProbe, NCH, NanoWorld, Neuchâtel, Switzerland) in air in the tapping mode. The typical settings of the AFM observations were as follows: a drive amplitude of 1.0−1.3 V, a set point of 0.95−1.25 V, and a scan rate from 1.80 to 3 Hz. The AFM images obtained are presented without any image processing except flattening.

3. Results and Discussion

At first, we discuss the behavior of the PMMA/PNA blend system, and then that of the PMMA-*b*-PNA block copolymer will be discussed.

3.1. PMMA/PNA Mixtures. *3.1.1. $\pi-A$ Isotherms of Monolayers of PMMA/PNA Mixtures.* In Figure 1, $\pi-A$ isotherms of PMMA, PNA, and PMMA/PNA mixtures (25/75, 50/50, and 75/25 in weight fraction) are shown. The PMMA monolayer (red line) showed a condensed-type $\pi-A$ isotherm without any clear transition, and it collapsed at a relatively high surface pressure around 50 mN/m. The PNA monolayer (blue line) also showed a condensed-type $\pi-A$ isotherm, but it collapsed at a lower surface pressure around 20 mN/m, which resembled a plateau transition. On the other hand, PMMA/PNA mixtures showed clear plateau transitions. PMMA/PNA mixtures with the PMMA content

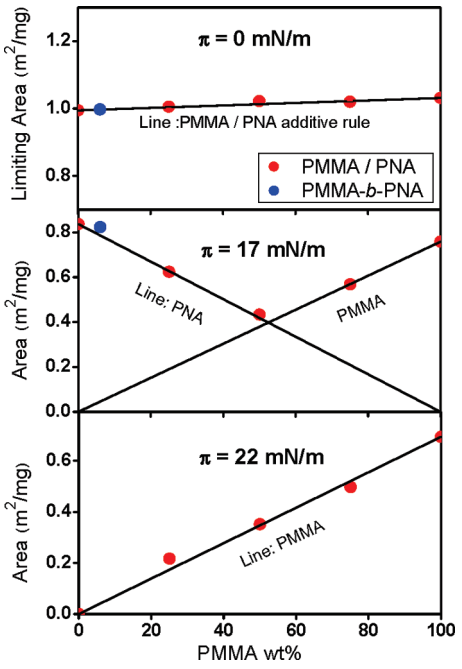

Figure 2. Plots of the limiting area (π = 0 mN/m) and areas at 17 and 22 mN/m derived from the $\pi-A$ isotherms in Figure 1 as a function of the PMMA weight content of the monolayers. The areas are in good agreement with the estimated lines, assuming that (i) the area at π = 0 mN/m was occupied by both PMMA and PNA monolayers obeying the additive rule, (ii) the area at π = 17 mN/m was occupied by either the PNA or PMMA monolayer depending on which was the major component, and (iii) the area at π = 22 mN/m was occupied by only the PMMA component.

higher than or equal to 50 wt %, PMMA/PNA = 50/50 (black line) and 75/25 (green), had a single plateau transition around 15 mN/m, while a mixture with a PMMA content less than 50 wt %, PMMA/PNA = 25/75 (orange line), showed two plateau transitions at around 16 and 20 mN/m.

In order to understand these $\pi-A$ isotherms, the limiting areas (extrapolated to π = 0), the areas after the first plateau transition (π = 17 mN/m), and the areas after the second plateau transition (π = 22 mN/m) derived from the $\pi-A$ isotherms were plotted against the PMMA content in Figure 2 (red circles). At 0 mN/m, the limiting areas of the PMMA/PNA mixtures were almost constant and agreed with areas estimated assuming an additive rule of the areas of pure PMMA and PNA monolayer (solid line in Figure 2 (0 mN/m)), indicating that both PMMA and PNA spread on the water surface. At 17 mN/m, after the first plateau transition, the area decreased linearly with the PMMA content up to 50 wt % but then rose linearly at PMMA contents of more than 50 wt %. The lines in 17 mN/m panel were estimated assuming that only the PNA or PMMA component occupied the water surface, ignoring the other component (solid lines of PNA and PMMA in Figure 2 (17 mN/m)). The results were in good agreement with this assumption, indicating that the monolayers at 17 mN/m were covered by either the PNA or PMMA monolayer depending which component was in the majority. At 22 mN/m after the second plateau transition, the areas linearly increased with the PMMA content and were in good agreement with a line estimated by assuming that only the PMMA monolayer covered the area on the water surface, ignoring the PNA component (solid line of PMMA in Figure 2 (22 mN/m)).

On the basis of the $\pi-A$ isotherm results and the AFM images of monolayers deposited on mica which we will show in the next section, we propose that the phase transition of the PMMA/PNA blends on the water surface proceed as

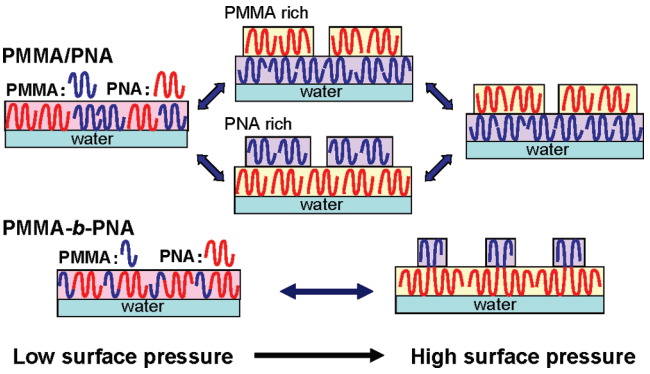

Figure 3. Schematic representation of the hierarchical phase separation of monolayers of PMMA and PNA mixtures and PMMA-*b*-PNA.

shown schematically in Figure 3. At a low surface pressure (1 mN/m), PMMA/PNA mixed monolayers are miscible and both the PMMA and PNA spread on the water surface. At 17 mN/m, the major component spread on the water surface as a monolayer, on top of which the minor component separated out, forming a hierarchical phase separation. At 22 mN/m, irrespective of the composition of the PMMA/PNA mixture, the PMMA component forms a monolayer on which PNA component separated out.

In the absence of detailed experimental evidence, readers may not fully agree with this picture at this moment. We now present further experimental evidence which supports the model described above.

3.1.2. AFM of Monolayers of PMMA/PNA Mixtures. Figure 4 shows tapping-mode AFM height images of monolayers of the PMMA/PNA mixtures (25/75, 50/50, and 75/25 w/w) deposited on mica at 1, 17, and 22 mN/m. At 1 mN/m, all the monolayers were homogeneous, and no clear phase separation was observed. The surface was quite smooth, and the surface roughness was less than 0.6 nm. In contrast, at 17 mN/m, immediately after the first plateau transition, all mixtures showed phase-separated structures. Although the phase separation of PMMA/PNA = 75/25 was small and thin relative to those of other compositions, the phase separation was obvious in comparison with the monolayer of the same composition deposited at 1 mN/m. On the basis of the $\pi-A$ isotherm results (Figures 2 and 3), we believe that at 17 mN/m the monolayers were occupied only by the PNA component for PMMA/PNA = 25/75 and only by the PMMA component for 50/50 and 75/25 mixtures. Thus, the upper (brighter) layer separated out on the monolayer was identified as PMMA for 25/75 and PNA for 50/50 and 75/25 mixtures. Further compression to 22 mN/m developed the phase separation. The size and height of the upper domains increased. From the $\pi-A$ isotherm results (Figures 2 and 3), we expect that all the monolayers were occupied by the PMMA component, and the upper layers separated out on the PMMA monolayer should be PNA for the all compositions at 22 mN/m. Since the lower monolayer was composed of a PMMA monolayer, increasing the PNA content led to a significant increase in the height of the separated-out PNA domain on the PMMA monolayer at 22 mN/m (1.4, 2.8, and 36 nm for PMMA/PNA = 75/25, 50/50, and 25/75 w/w, respectively).

As shown in the schematic representation of the hierarchical phase separation in Figures 3 and 4, the hierarchical phase separation of PMMA/PNA = 50/50 and 75/25 mixture maintained a layer structure with a lower PMMA monolayer and an upper PNA layer from 17 to 22 mN/m. In contrast, the hierarchical phase separation of the PMMA/PNA = 25/75 mixture must exchange the upper and lower layer

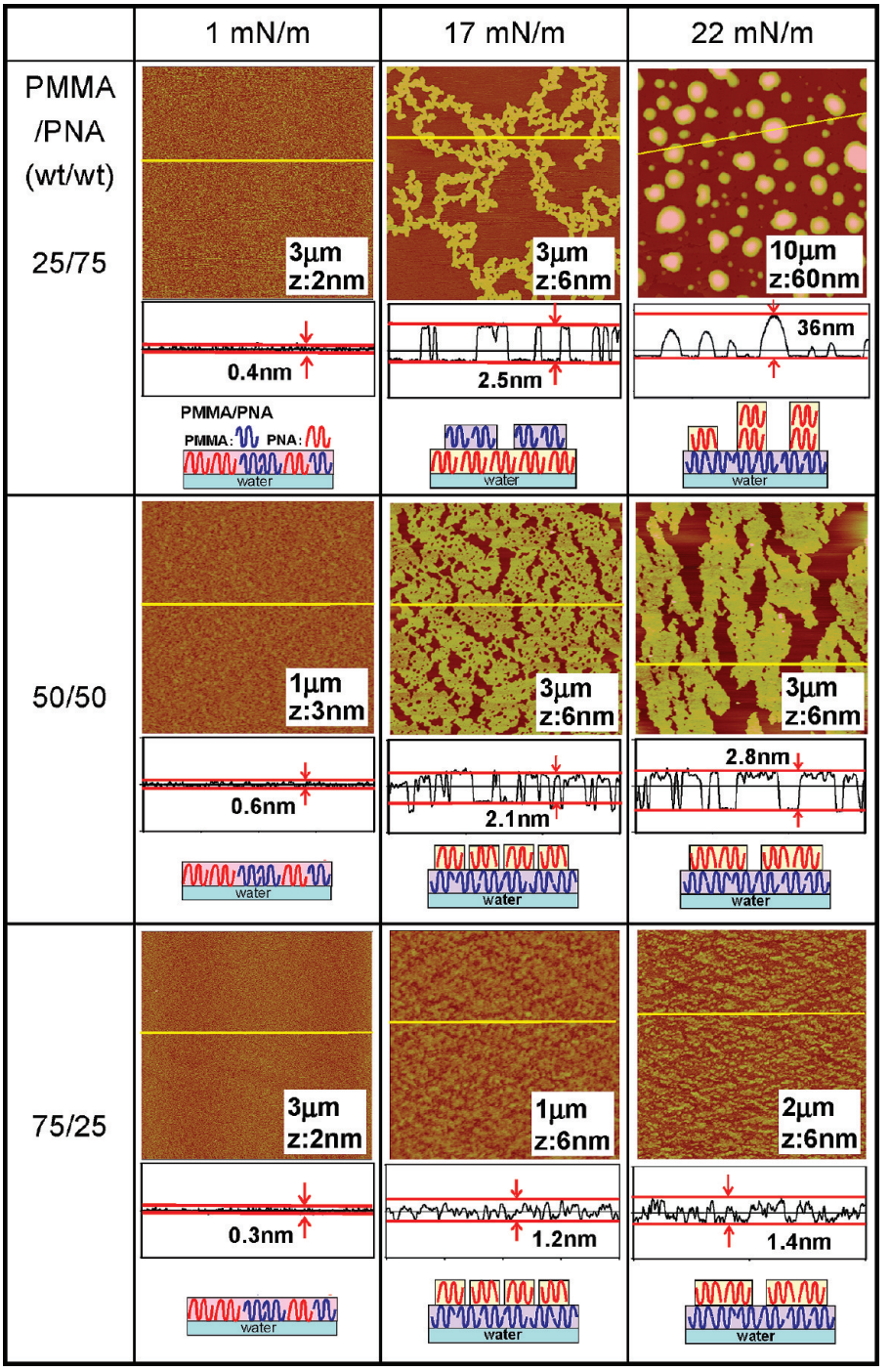

Figure 4. Tapping-mode AFM height images of the monolayers of PMMA/PNA mixtures (25/75, 50/50, and 75/25 in weight fraction) deposited on mica at a surface pressure of 1, 17, and 22 mN/m. Height profiles along the yellow lines in the images are also shown. The width and *z*-range of the images are indicated in each image. Schematic representations of the hierarchical phase separation of the mixed monolayers are also shown.

during the compression from 17 to 22 mN/m. Evidence of this inversion of the upper PMMA layer and lower PNA monolayer of PMMA/PNA = 25/75 during the compression was derived mainly from the area occupied at the surface pressures in the $\pi-A$ isotherms (Figure 2). This inversion of the hierarchical phase separation is peculiar and needs confirmation. Accordingly, in the next section, we report observations of the phase inversion behavior of the PMMA/PNA = 25/75 mixture during the compression from 17 to 22 mN/m in more detail.

3.1.3. Inversion of Upper and Lower Layers during Compression of PMMA/PNA = 25/75 Mixture from 17 to 22 mN/m. Figure 5A shows AFM height images of a monolayer of the PMMA/PNA = 25/75 deposited on mica at the surface pressures indicated in the images and in the $\pi-A$ isotherms of Figure 5B(1−6). As mentioned, the $\pi-A$ isotherm of the PMMA/PNA = 25/75 showed two plateau transitions. Immediately after the first transition at 17 mN/m (1), on the basis of the occupied area, we assumed that a PNA monolayer covered the water surface on top of which the PMMA layer separated out. Thus, the brighter region with a thickness around 2.5 nm was a PMMA layer deposited on the PNA monolayer. At the onset of the second plateau of the $\pi-A$ isotherm ((2) 19 mN/m), a small number of thicker areas

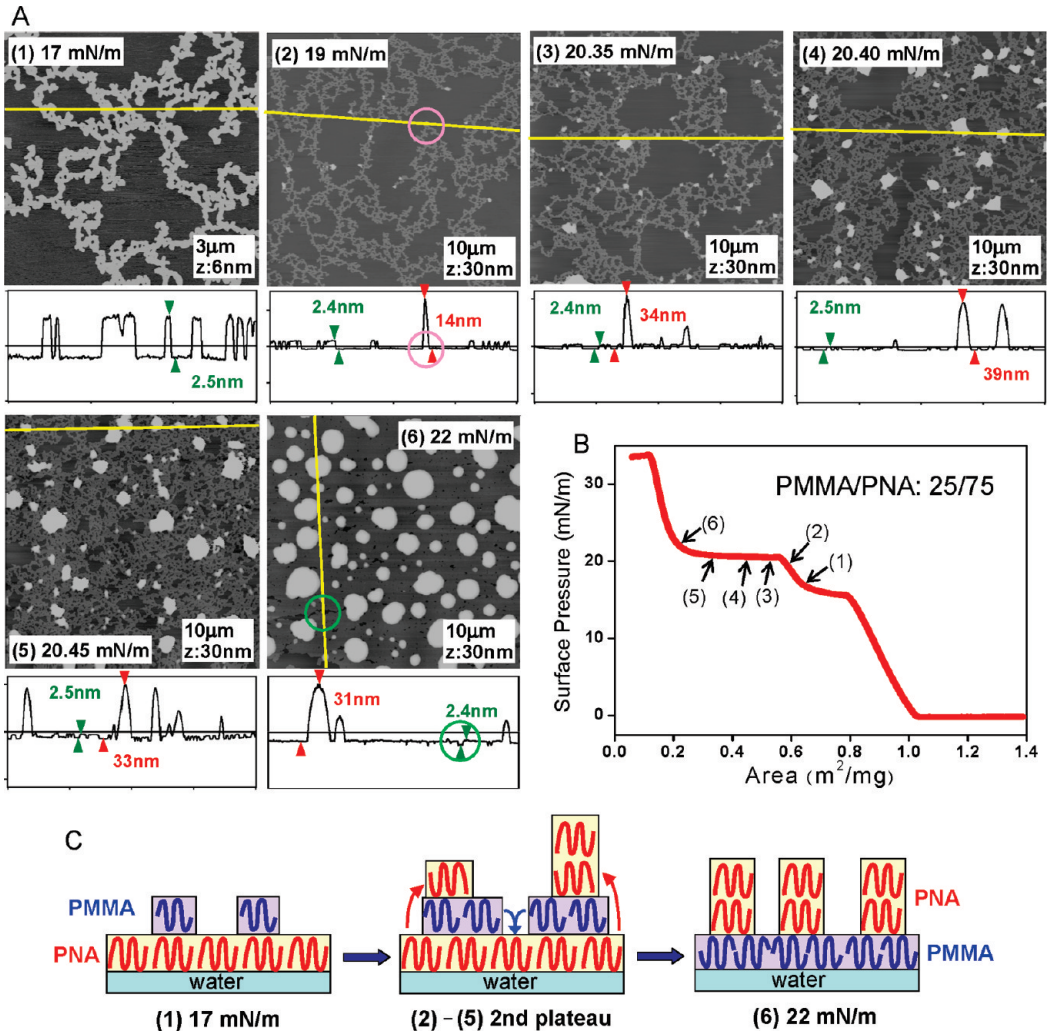

Figure 5. (A) Tapping-mode AFM height images of the monolayers of a PMMA/PNA mixture (25/75 w/w) deposited on mica at surface pressures indicated in the images. Height profiles along the yellow lines in the images are also shown. The width and *z*-range of the images are indicated in each image. (B) The $\pi-A$ isotherm of the monolayer of PMMA/PNA (25/75 w/w). The areas at the monolayers were deposited are indicated by the arrows. (C) Schematic representation of a possible inversion mechanism of the hierarchical phase separation of the monolayer.

appeared on top of the PMMA layer; for example, see domains with a thickness of 14 nm in a pink circle in Figure 5A(2). During the second plateau, the diameter and height of the thicker depositions increased. Note that the new thicker domains were selectively deposited on the PMMA domains (Figure 5A(2−5)). These newly deposited domains on the PMMA layer should be PNA collapsing at its collapse surface pressure around 20 mN/m. During the second plateau, the area occupied by the PMMA layer increased, and at the end of the plateau at 22 mN/m (6), an almost homogeneous PMMA monolayer covered the surface. This is in good agreement with the $\pi-A$ isotherm analysis mentioned above, which indicated at 22 mN/m the area was covered only by the PMMA monolayer without any PNA contribution (Figure 2). The thickness of the PMMA monolayer determined at a crack shown in a green circle in Figure 5A(6) was 2.4 nm, indicating the thickness of the PMMA monolayer was almost constant throughout the compression from 17 to 22 mN/m (2.4−2.5 nm, green arrows in Figure 5A(1−6)). In Figure 5C, a possible inversion process is schematically shown.

3.1.4. Assignment of Upper and Lower Components in the Hierarchical Phase Separation. As already mentioned, the areas at 17 and 22 mN/m were covered only by a PNA or PMMA monolayer, the other component not contributing to these areas, and as a result, we thought the other component deposited on the monolayers. However, a skeptical reader may point out the possibility that the other component which did not contribute to the area may exist under the monolayer, i.e., not at the air/monolayer interface but at the monolayer/water interface of the other component. As we used AFM to observe the hierarchical phase separation of monolayers after they were deposited on a substrate, we must agree that it is hard to distinguish which domain was at the upper side solely by using AFM. However, we believe that we may reasonably assign the layer structure considering the nature of monolayers on the water surface as described below.

PMMA and PNA both have an appropriate hydrophilic group that allows them to spread on a water surface with the hydrophilic group adsorbing to the water surface to form a stable Langmuir monolayer. However, a Langmuir monolayer of PMMA or PNA is stable only on the water surface. If a monolayer deposits on a monolayer of the other component, the second monolayer is no longer a Langmuir monolayer and so is not necessarily stable and should behave differently from a normal Langmuir monolayer on a water surface. As mentioned, at 17 and 22 mN/m, the area was covered by a PNA or PMMA monolayer depending on the composition with no contribution from the other component. Thus, the PNA or PMMA monolayer should be spread on the water surface, on top of which the

other component separates out. If the other component existed under the monolayer, i.e., between the monolayer/water interface, the monolayer deposited on the other component would not be stable at that area and would not be able to withstand for the surface pressure.

Therefore, for example, in the PMMA/PNA = 25/75 composition at 17 and 22 mN/m, we suppose that the water surface was covered with a PNA and PMMA monolayer, respectively, with other component deposited on that monolayer. Moreover, the $\pi-A$ isotherm for the PMMA/PNA = 25/75 composition in Figure 5A has two plateau transitions. After the first plateau, which corresponds to deposition of the PMMA component on the PNA monolayer, the resultant $\pi-A$ isotherm (from (1) to (6) in Figure 5B) was quite similar to that of the monolayer of pure PNA (blue line in Figure 1), taking into consideration a reduction of the area due to the composition of the blend (75 wt % of PNA). After the second plateau, which corresponded to deposition of the PNA on the PMMA monolayer, the resultant $\pi-A$ isotherm (from (6) to the end in Figure 5B) was, again, quite similar to that of the monolayer of pure PMMA (red line in Figure 1), again allowing for a reduction of the area due to the composition of the blend (25 wt % of PMMA). The agreement of the $\pi-A$ isotherms after deposition of the other component strongly indicates that the other component separated out on top of the monolayer spread on the water surface. The inversion of the monolayer of PMMA/PNA = 25/75 composition is quite peculiar, but the development of the phase-separated structure observed by AFM and the $\pi-A$ isotherm behavior support the inversion of the monolayer of this composition.

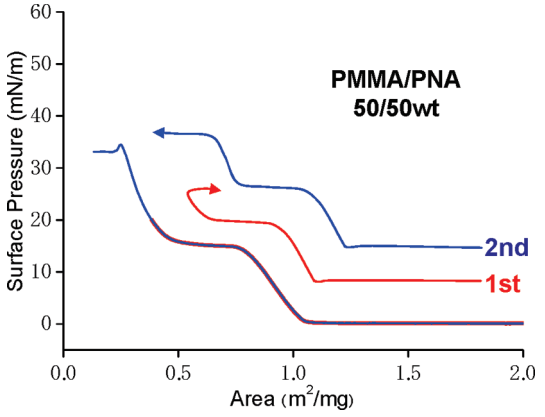

Figure 6. Reversible $\pi-A$ isotherm of the monolayer of the PMMA/PNA mixture (PMMA/PNA = 50/50 w/w). The monolayer was first compressed up to 20 mN/m (red line), then immediately expanded to 0 mN/m (2.0 m^2/mg), and again immediately compressed (blue line).

The $\pi-A$ isotherms of PMMA/PNA = 50/50 and 75/25 had a single plateau transition, and after the transition the resultant $\pi-A$ isotherms were, again, quite similar to that of the pure PMMA (red line in Figure 1) considering the composition of the blend (50 and 75 wt % of PMMA). This result indicates that after the transition a PMMA monolayer spread on the water surface with the PNA deposited on that monolayer. In addition, the $\pi-A$ isotherms of the 50/50 and 75/25 compositions which showed a single plateau transition (Figure 1) indicated no particular sign of inversion of the hierarchical phase separation, as was observed in the PMMA/PNA = 25/75 composition.

3.1.5. Reversibility of Hierarchical Phase Separation of PMMA/PNA Blend Monolayer. A question arises: are these hierarchical phase separations a reversible process? Figure 6 shows the $\pi-A$ isotherm of a PMMA/PNA = 50/50 mixture measured during the first compression up to 20 mN/m (red line: first compression), then immediately expanded to 2.0 m^2/mg (0 mN/m), and again immediately compressed until collapse (blue line: second compression). The $\pi-A$ isotherms of the first and second compressions (red and blue lines in Figure 6) were identical, indicating the monolayer compressed up to 20 mN/m recovered to the original structure on the subsequent expansion to 0 mN/m. Thus, the hierarchical phase separation was indeed reversible.

In addition, Figure 7 shows AFM height images of a monolayer of a PMMA/PNA mixture (50/50 w/w) deposited on mica during a compression−expansion−compression cycle.

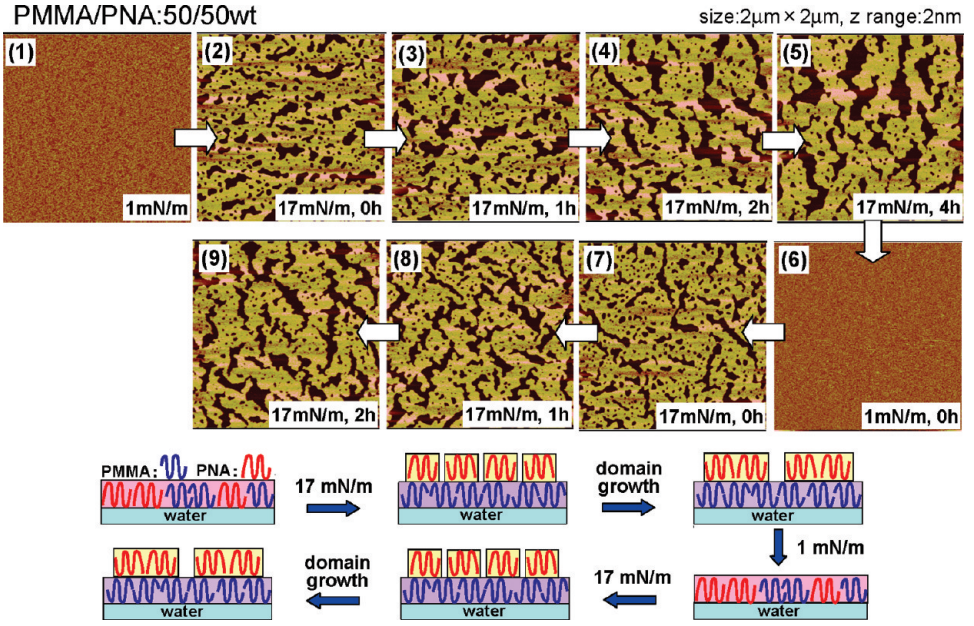

Figure 7. Tapping-mode AFM height images of the monolayer of a PMMA/PNA mixture (50/50 w/w) deposited on mica during a compression−expansion−compression cycle. The monolayer was first compressed to 1 mN/m (1), further compressed to 17 mN/m (2), then kept at the surface pressure for 4 h (3−5), next expanded to 1 mN/m (6), again compressed to 17 mN/m (7), and kept at the surface pressure for 2 h (8−9). A schematic representation of the hierarchical phase separations of the mixed monolayer during the compression−expansion−compression cycle is also shown.

The monolayer was first deposited at 1 mN/m (1), further compressed to 17 mN/m (2), and kept at that surface pressure for 4 h (3−5), next expanded to 1 mN/m (6), then immediately compressed to 17 mN/m (7), and kept at that surface pressure for 2 h (7−9). The monolayer was homogeneous at 1 mN/m (1). Further compassion up to 17 mN/m resulted in a hierarchical phase separation with a PMMA monolayer on which a PNA separated out. The domain of PNA deposited layer on the PMMA monolayer grew with time (2−5). However, subsequent expansion immediately resulted in the disappearance of the hierarchical phase separation into a homogeneous monolayer (6) similar to that before compression (1). Subsequent compression immediately recovered a hierarchical phase separation (7), and the domain size of the deposited PNA grew with time (7−9). Note that the recovered PNA domain at 0 h (7) was similar to that formed immediately after the first compression to 17 mN/m (2) and not identical to that immediately before the expansion ((5) after 4 h at 17 mN/m). Furthermore, the growth of the deposited PNA domain at the second compression at 17 mN/m (7−9) was quite similar to that of the first compression at 17 mN/m (2−4). This strongly indicates that the monolayer (6), which was expanded after being phase separated at 17 mN/m for 4 h, did not simply appear to be homogeneous but was truly in a miscible state. A schematic representation of the phase separation is shown in Figure 7.

In consequence, the PMMA/PNA monolayer is truly miscible at lower surface pressures, and it hierarchically phase separates at a higher surface pressure. The hierarchical phase separation is reversible as a function of the surface pressure; thus, the phase separation is a true thermodynamic transition.

3.1.6. Discussion of the Composition-Dependent Inversion of the Hierarchical Phase Separations. As previously mentioned, at 17 mN/m the PMMA/PNA blend monolayers underwent a hierarchical phase separation, with the major component spread as a monolayer, on top of which the minor component separated out. The lower monolayer was PNA for the PMMA/PNA = 25/75 blend and PMMA for the 50/50 and 75/25 blends, respectively. Why was the monolayer different depending on the composition? There are six different surface/interface tension coefficients that characterize spreading of the blend on the water surface. They are surface/interface tensions of the water/air (γ_{water}), PMMA/water ($\gamma_{PMMA/water}$), PMMA/air ($\gamma_{PMMA/air}$), PNA/water ($\gamma_{PNA/water}$), PNA/air ($\gamma_{PNA/air}$), and PMMA/PNA ($\gamma_{PMMA/PNA}$) interfaces. Using these coefficients, four spreading coefficients can be estimated that characterize spreading of PMMA monolayer on the water surface ($S_{PMMA/water}$), PNA monolayer on the water surface ($S_{PNA/water}$), PMMA on the PNA monolayer ($S_{PMMA/PNA}$), and PNA on the PMMA monolayer ($S_{PNA/PMMA}$) as follows:[28]

$$S_{PMMA/water} = \gamma_{water} - \gamma_{PMMA/water} - \gamma_{PMMA/air}$$

$$S_{PNA/water} = \gamma_{water} - \gamma_{PNA/water} - \gamma_{PNA/air}$$

$$S_{PMMA/PNA} = \gamma_{PNA/air} - \gamma_{PMMA/PNA} - \gamma_{PMMA/air}$$

$$S_{PNA/PMMA} = \gamma_{PMMA/air} - \gamma_{PMMA/PNA} - \gamma_{PNA/air}$$

Since both the PMMA and PNA formed stable monolayers on the water surface, $S_{PMMA/water}$ and $S_{PNA/water}$ should be positive. If there were significant difference in magnitude between the two values, a monolayer of the material with the larger spreading coefficient would spread on the water surface, on top of which the other component with the smaller spreading coefficient would separate out irrespective of the blend composition, since it is thermodynamically favorable. This was not the case. Therefore, we expect that $S_{PMMA/water}$ and $S_{PNA/water}$ are comparable, and the lower monolayer was either PMMA or PNA depending on which was the major component of a mixture. The spreading coefficient, $S_{A/B}$, corresponds to the energy gain to form A/B interface per unit area. In the case that $S_{PMMA/water}$ and $S_{PNA/water}$ are comparable, the energy to peel off a monolayer of the minor component from the water surface is smaller than the opposite case; therefore, the minor component should separate out.

To be more accurate, we need to consider additional factors required to form a PMMA/PNA or PNA/PMMA interface to construct a hierarchical phase separation, but if $S_{PMMA/PNA}$ and $S_{PNA/PMMA}$ are comparable, the above argument works qualitatively. As shown in Figure 7, the PNA domains that separated out on the PMMA monolayer grew with the elapsed time; in other words, the PNA slowly dewetted. Therefore, $S_{PNA/PMMA}$ should be negative. Also, $S_{PMMA/PNA}$ is expected to be negative, based on the dewetting behavior of PNA domains on the PMMA monolayer in Figure 5(2−6).

3.1.7. Discussion of the Phase Inversion of the Hierarchical Phase Separation of the PMMA/PNA = 25/75 Mixture during the Second Transition. As shown in Figure 5, at the first transition, the PMMA/PNA mixture at first formed a hierarchical phase separation with a lower PNA monolayer on which PMMA deposited, but further compression resulted in a second transition in which a phase inversion occurred to form a new hierarchical phase separation with a lower PMMA monolayer on which PNA deposited. This raises the question: why did this phase inversion at 22 mN/m occur after the formation of the thermodynamically stable hierarchical phase separation of the first transition?

The inversion occurs because of the collapse of the PNA monolayer at its collapse pressure. The PNA monolayer was no longer stable at 22 mN/m and collapsed. On the other hand, at 22 mN/m, PMMA could adsorb on the water surface and form a stable monolayer; thus, PNA was excluded on the PMMA monolayer, resulting in the inverted hierarchical phase separation. After the first transition, the PMMA/PNA mixture had already undergone a hierarchical phase separation; therefore, the second transition occurred at the same surface pressure as the collapse pressure of the pure PNA, with no effect on the PMMA component (Figure 1, orange and blue lines). On the other hand, the surface pressure of the first transition where the hierarchical phase separation formed from the miscible blends clearly depended on the composition of the blends (Figure 1, green, black, and orange lines).

Figure 8 shows a phase diagram of the hierarchical phase separation of the PMMA/PNA mixtures (red circle). The points were determined based on the inflection points of the $\pi-A$ isotherms of the blends. The surface pressure at the phase transition depends on the composition of the blends.

3.2. PMMA-*b*-PNA Block Copolymer. *3.2.1. $\pi-A$ Isotherm and AFM Image of Monolayer of PMMA-b-PNA Block Copolymer*. Next, we move to a PMMA-*b*-PNA block copolymer system. The M_n for the PMMA and PNA blocks were 1.3×10^4 and 2.03×10^5, respectively, and the PMMA content was about 6 wt %. The $\pi-A$ isotherm of the PMMA-*b*-PNA is shown in Figure 1A (pink line). As the PMMA content was small, the $\pi-A$ isotherm of the PMMA-*b*-PNA was similar to that of the PNA homopolymer (blue line in Figure 1A), but the surface pressure at collapse was slightly higher. Furthermore, as shown in the magnified $\pi-A$ isotherms in Figure 1B, a small inflection around 17 mN/m (pink arrow) of the $\pi-A$

isotherm of the PMMA-*b*-PNA (pink line) indicates deposition of the PMMA block onto the monolayer of PNA block. In contrast, the PNA homopolymer without a PMMA component did not show this transition (blue line in Figure 1B). The limiting area and area at 17 mN/m are plotted in Figure 2 (blue circles), the behavior of which was similar to those of the PMMA/PNA blend monolayers.

AFM height images of the monolayer of the PMMA-*b*-PNA deposited on mica at surface pressures of 1, 10, and 20 mN/m are shown in Figure 9. The monolayer was again homogeneous at 1 mN/m, at 10 mN/m a slight increase in roughness was recognizable, and at 20 mN/m a relatively homogeneous distribution of dots with a thickness about 2.5 nm was observed. By analogy with the PMMA/PNA system with a PMMA minor composition, the dots were identified as PMMA blocks deposited on a monolayer of PNA block. The size was relatively homogeneous, and the dot−dot distance was also relatively constant, which is expected to be controlled by the monolayer of the PNA block beneath the PMMA dots. Each of the dots is composed of about 29 PMMA blocks on average, as calculated from the number of the polymer chains that existed in the image based on the LB deposition conditions, $N_{\text{block copolymer}}$, and the number of the dots, N_{dot}, as $N_{\text{block copolymer}}/N_{\text{dot}}$.

3.2.2. Reversibility of Monolayer of PMMA-b-PNA Block Copolymer. Figure 10 shows a $\pi-A$ isotherm of the PMMA-*b*-PNA block copolymer measured during the first compression until 0.5 m^2/mg (red line: first compression), then immediately expanded to 2.0 m^2/mg (0 mN/m), and again recompressed to collapse (blue line: second compression). The second compression exactly traced the $\pi-A$ isotherm of the first compression, indicating that the hierarchical phase separation was reversible.

Figure 11 shows AFM height images of the monolayer of the PMMA-*b*-PNA block copolymer deposited during a compression−expansion−compression cycle. The monolayer was first deposited at 10 mN/m (1), further compressed to 20 mN/m (2), kept at that surface pressure for 2 h (3−6), then expanded to 10 mN/m (6), kept at that surface pressure

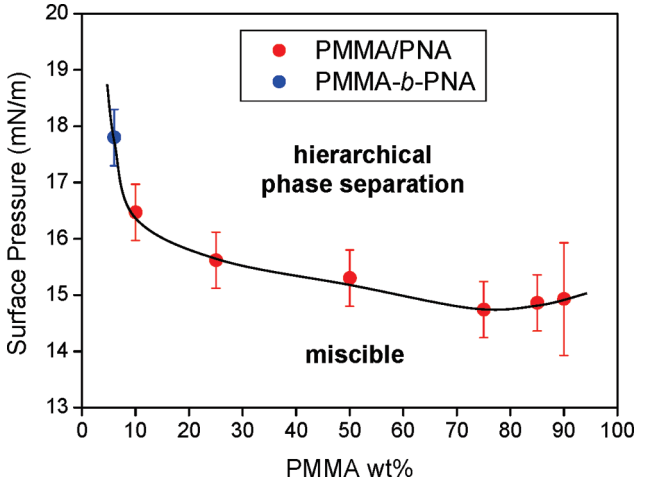

Figure 8. Phase diagram of the hierarchical phase separation of the PMMA/PNA mixtures (red circle) and the PMMA-*b*-PNA (blue circle). The points were determined based on the inflection points of the $\pi-A$ isotherms for the corresponding compositions.

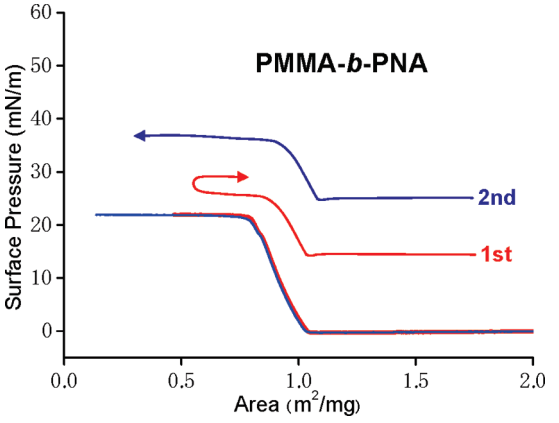

Figure 10. Reversible $\pi-A$ isotherm of a PMMA-*b*-PNA monolayer. The monolayer was first compressed up to 22 mN/m (red line), then immediately expanded to 0 mN/m (2.0 m^2/mg), and again, immediately compressed (blue line).

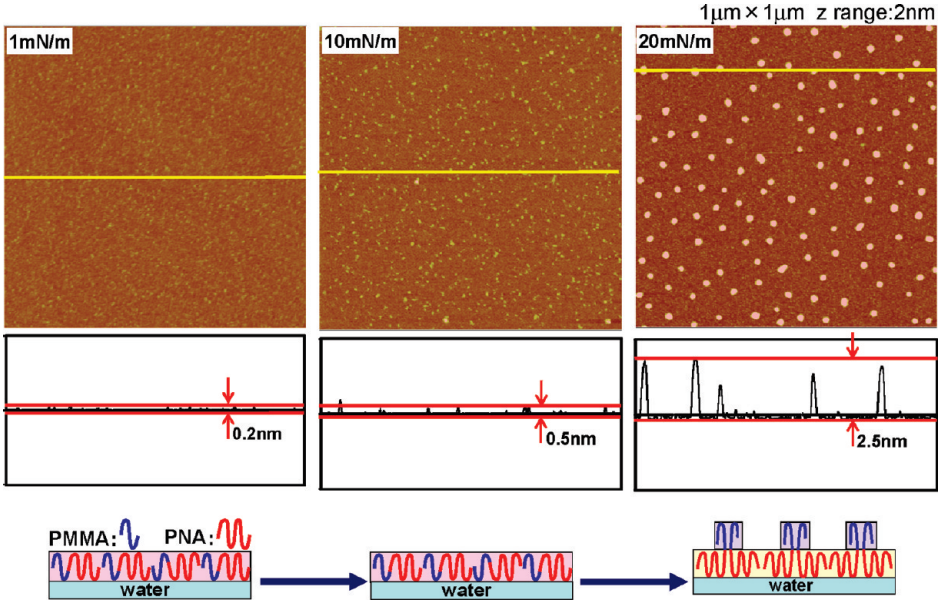

Figure 9. Tapping-mode AFM height images of a monolayer of PMMA-*b*-PNA deposited on mica at a surface pressure of 1, 10, and 20 mN/m. Height profiles along the yellow lines in the images are also shown. A schematic representation of the hierarchical phase separation of the PMMA-*b*-PNA monolayer is also shown.

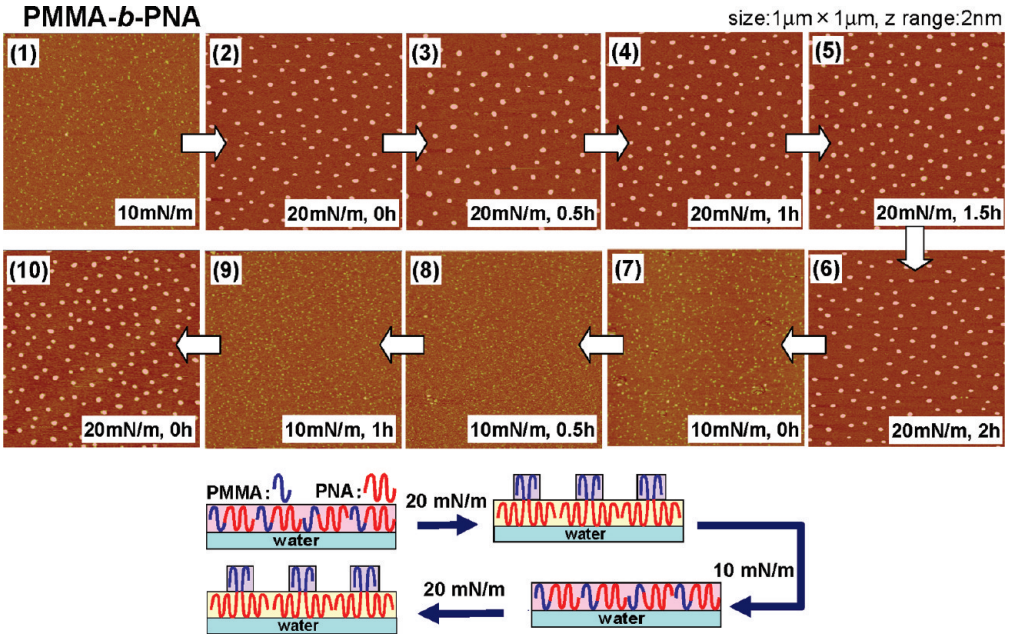

Figure 11. Tapping-mode AFM height images of a PMMA-*b*-PNA monolayer deposited on mica during a compression−expansion−compression cycle. The monolayer was first compressed to 10 mN/m (1), further compressed to 20 mN/m (2), then kept at the surface pressure for 2 h (3−6), next expanded to 10 mN/m (7), kept at the surface pressure for 1 h (8−9), and then again compressed to 20 mN/m (10). A schematic representation of the hierarchical phase separations of the PMMA-*b*-PNA monolayer during the compression−expansion−compression cycle is also shown.

for 1 h (7−9), and finally recompressed to 20 mN/m (10). The monolayer was miscible at 10 mN/m (1), and further compression up to 20 mN/m resulted in a hierarchical phase separation with small domains of the PMMA block deposited on top of the monolayer of PNA block (2). As expected for a phase separation of a block copolymer system, the resultant phase separation structure of the PMMA-*b*-PNA was stable and did not change with time at 20 mN/m for 2 h (2−6), in contrast to the hierarchical phase separation of PMMA/PNA blend systems which grew with time (Figure 7). Expansion to 10 mN/m immediately resulted in disappearance of the phase separation and produced a miscible monolayer (7) which was stable at 10 mN/m for 1 h (7−9). Recompression to 20 mN/m immediately resulted in recovery of the hierarchical phase separation (10). Therefore, the hierarchical phase separation is a reversible process, and we can conclude that it is a true thermodynamic transition. In Figure 8, the surface pressure at the hierarchical phase separation determined from the inflection point of the $\pi-A$ isotherm of the block copolymer (blue circle) was added to the phase diagram of the PMMA/PNA blends.

We note that the hierarchical phase separation of the PMMA-*b*-PNA formed through a thermodynamic transition from the miscible state. Thus, the resultant structure is expected to be close to a thermodynamically stable structure of the PMMA-*b*-PNA. This situation is not usually attained for block copolymers spread on a water surface; thus, the present system is suitable for studying the equilibrium structure and the construction of well-organized structures using block copolymers.[29]

4. Concluding Remarks

Mixed monolayers composed of PMMA and PNA were miscible at a lower surface pressure but underwent a reversible hierarchical phase separation at a higher surface pressure, with the monolayer of the major component being spread on the water surface, on top of which the minor component separated out. AFM observation of the monolayer in addition to $\pi-A$ isotherm measurements clarified the behavior of the hierarchical phase separation. Polymer blend monolayers studied in detail by AFM are still very limited and need to be studied by this technique in addition to $\pi-A$ isotherm measurements. The study of polymer blend monolayers is important not only for the control of polymer thin films but also to improve our understanding of the nature of polymer in 2D states.

Acknowledgment. This work was supported by a Grant-in-Aid for Scientific Research on Innovative Areas (20106009) and Scientific Research (B) (21350059) from the Ministry of Education, Culture, Sports, Science, and Technology, Japan.

References and Notes

(1) (a) Crisp, D. J. *J. Colloid Interface Sci.* **1946**, *1*, 49–70. (b) Gaines, G. L., Jr. *Insoluble Monolayers at Liquid-Gas Interfaces*; Interscience: New York, 1966. (c) Ulman, A. *An Introduction to Ultrathin Organic Films: From Langmuir-Blodgett to Self-Assembly*; Academic Press: New York, 1991.
(2) Wu, S.; Huntsberger, J. R. *J. Colloid Interface Sci.* **1969**, *29*, 138–147.
(3) Labbauf, A.; Zack, J. R. *J. Colloid Interface Sci.* **1970**, *35*, 569–583.
(4) Gabrielli, G.; Puggelli, M.; Faccioli, R. *J. Colloid Interface Sci.* **1971**, *37*, 213–218.
(5) Gabrielli, G.; Puggelli, M.; Faccioli, R. *J. Colloid Interface Sci.* **1973**, *44*, 177–180.
(6) Gabrielli, G.; Puggelli, M.; Ferroni, E. *J. Colloid Interface Sci.* **1974**, *47*, 145–154.
(7) Gabrielli, G.; Baglioni, P. *J. Colloid Interface Sci.* **1980**, *73*, 582–587.
(8) Gabrielli, G.; Puggelli, M.; Baglioni, P. *J. Colloid Interface Sci.* **1982**, *86*, 485–500.
(9) Caminati, G.; Gabrielli, G.; Puggelli, M.; Farroni, E. *Colloid Polym. Sci.* **1989**, *267*, 237–245.
(10) Kawaguchi, M.; Nishida, R. *Langmuir* **1990**, *6*, 492–496.
(11) Kawaguchi, M.; Nagata, K. *Langmuir* **1991**, *7*, 1478–1482.
(12) Kawaguchi, M.; Suzuki, S.; Imae, T.; Kato, T. *Langmuir* **1997**, *13*, 3794–3799.
(13) Yamamoto, S.; Tsujii, Y.; Fukuda, T. *Polymer* **2001**, *42*, 2007–2013.
(14) Aoki, H.; Kunai, Y.; Ito, S.; Yamada, H.; Matsushige, K. *Appl. Surf. Sci.* **2002**, *188*, 534–538.

(15) Kawaguchi, M.; Suzuki, M. *J. Colloid Interface Sci.* **2005**, *288*, 548–552.
(16) Ohkita, M.; Higuchi, M.; Kawaguchi, M. *J. Colloid Interface Sci.* **2005**, *292*, 300–303.
(17) Lee, Y.-L.; Hsu, W.-P.; Lio, S.-H. *Colloids Surf., A* **2006**, *272*, 37–47.
(18) Li, B.; Marand, H.; Esker, A. R. *J. Polym. Sci., Part B: Polym. Phys.* **2007**, *45*, 3200–3318.
(19) Hsu, W.-P.; Li, H.-Y.; Chiou, M.-S. *Colloids Surf., A* **2009**, *335*, 73–79.
(20) Aiba, N.; Sasaki, Y.; Kumaki, J. *Langmuir* **2010**, *26*, 12703–12708.
(21) de Gennes, P.-G. *Scaling Concepts in Polymer Physics*; Cornell University Press: Ithaca, NY, 1979; pp 60−61.
(22) Kumaki, J.; Kawauchi, T.; Yashima, E. *J. Am. Chem. Soc.* **2005**, *127*, 5788–5789.
(23) Kumaki, J.; Kawauchi, T.; Okoshi, K.; Kusanagi, H.; Yashima, E. *Angew. Chem., Int. Ed.* **2007**, *46*, 5348–5351.
(24) Kumaki, J.; Kawauchi, T.; Ute, K.; Kitayama, T.; Yashima, E. *J. Am. Chem. Soc.* **2008**, *130*, 6373–6380.
(25) Kawauchi, T.; Kumaki, J.; Kitaura, A.; Okoshi, K.; Kusanagi, H.; Kobayashi, K.; Sugai, T.; Shinohara, H.; Yashima, E. *Angew. Chem., Int. Ed.* **2008**, *47*, 515–519.
(26) Kumaki, J.; Kajitani, T.; Nagai, K.; Okoshi, K.; Yashima, E. *J. Am. Chem. Soc.* **2010**, *132*, 5604–5606.
(27) Kumaki, J.; Sakurai, S.-i.; Yashima, E. *Chem. Soc. Rev.* **2009**, *38*, 737–746.
(28) Palyukova, E. S.; Polemkin, I. I. *Langmuir* **2007**, *23*, 12356–12365.
(29) The exception is a polystyrene-*b*-poly(4-vinylpyridine) (PS-*b*-P4VP) monolayer studied by Nagano and Seki. They succeeded to form hierarchical phase separation of the PS-*b*-P4VP with a P4VP monolayer on which regular PS domains deposited, by cospreading a polar liquid crystal molecule, 4′-pentyl-4-cyanobiphenyl (5CB) with the PS-*b*-4VP on a water surface. The 5CB behaved as a "molecular solvent", and at a low surface pressure, it dissolved the PS-*b*-P4VP into a miscible state. Upon compression, the PS-*b*-P4VP underwent the hierarchical phase separation from the miscible state. See: Nagano, S.; Matsushita, Y.; Ohmuma, Y.; Shinma, S.; Seki, T. *Langmuir* **2006**, *22*, 5233–5236.